Formation of Nano-Sized Silver Particles during Thermal and Photochemical Decomposition of Silver Carboxylates

B. B. Bokhonov

Institute of Solid State Chemistry, Novosibirsk, Russia

L. P. Burleva and D. R. Whitcomb▲

Eastman Kodak Company, Oakdale, Minnesota

Yu. E. Usanov

Vavilov State Optics Institute, St. Petersburg, Russia

The changes in the morphology and structure of silver carboxylates during thermal and photochemical decomposition were investigated using TEM, x-ray diffraction, and DTA. Thermal and photochemical decomposition of long chain silver carboxylates were both found to form nano-sized silver particles (3–5 nm). This type of metallic silver formation can be directly attributed to the layered structure of the solid state structure of the $[Ag(O_2C_nH_{2n-1})]_2$ dimers in the crystalline lattice. In addition, this type of metallic silver was observed to be influenced by the organic by-products formed, which can hinder the addition of new silver atoms to the growing metal crystallite.

Journal of Imaging Science and Technology 45: 259–266 (2001)

Introduction

Silver carboxylates, having the general formula $[Ag(O_2C_nH_{2n-1})]_2$, where n = 10–22, are the primary sources of the metallic silver image in contemporary thermographic and photothermographic materials.[1,2] However, in spite of a series of reports on the morphology of silver particles formed during thermal development of photothermographic materials,[3–5] there is very little reported on the more general topic of the morphology and structure of the metallic silver particles formed during thermal and photochemical decomposition of pure silver carboxylate crystals. For example, earlier studies[6] of the changes in the morphology of the products formed in the photochemical decomposition of recrystallized silver stearate crystals, n = 18, involved the investigation of behaviour exhibited by the organic products of the reaction but did not consider the subject of the metallic silver phase formation.

The morphology and structure of silver behenate crystals during thermal decomposition have recently been explored.[7] However, the data presented in this work describes the formation of metallic silver particles but is generally limited to the size of the metallic silver crystals under various thermal processing conditions. For example, it was stated that the silver behenate crystals melt at 150°C and silver particles are formed everywhere, even outside the silver behenate crystal. These results contradict other reported data concerning the phase behavior of silver carboxylate crystals.[8,9] In addition, the formation of metallic silver crystallites outside the silver carboxylate crystal implies an ionic mobility not here-to-for discussed in the literature and requires special explanation.

Recently, due to the increasing commercial interest in thermographic and photothermographic imaging materials utilising silver carboxylates, new information on the thermal decomposition of silver behenate (n = 22) has been reported.[10,11] In one case, the focus is on the thermal phase transitions and the other with thermal decomposition within polyvinylbutyral films, but neither discuss the morphology of the metallic silver formed.

Photolysis of various other silver carboxylates, including high molecular weight silver carboxylates such as silver alginate or silver pectate, has focused on the formation of metal films for conductivity.[12–14] The photolytic silver formation is described by a diffusion model, which takes into account diffusion and deposition of silver atoms and clusters. Three parameters, a photolytic silver formation time constant (1000 sec), a deposition rate constant in the film (10^{-3}/sec), and a diffusion coefficient (10^{-1} cm^2/sec) describe the photochemical formation of the metallic silver deposit. While the model applies to the formation of either colloidal silver particles (room temperature photolysis) or large silver clusters (liquid nitrogen temperature photolysis) the results are focused on diffusion of silver ions from silver carboxylates dispersed in a polymer film.

Original manuscript received October 12, 2000

▲ IS&T Member

Information on the structure and morphology of metallic silver crystals formed during thermal and photochemical decomposition of silver carboxylates enables a better understanding of the mechanism by which pure silver carboxylates decompose. In addition, comparison of the known data on the morphology and structure of the metallic silver particles formed during the development of photothermographic materials[3,5,15] with that of the silver particles formed during thermal and photochemical decomposition of pure silver car-boxylates can provide further insight into the thermal development of the metallic silver image in these types of imaging materials.

Experimental

Silver carboxylates, $[Ag(O_2C_nH_{2n-1})]_2$ where n = 10, 12, 14, 16, 18, and 22, were prepared by the normal exchange reaction between the sodium salt of the corresponding fatty acid and silver nitrate under aqueous conditions using the procedure described previously.[15]

Thermal decomposition of silver carboxylates was carried out in a thermostatic cell at 110–180°C. Temperature was measured with an accuracy of ±1°C. Photochemical decomposition of the samples was carried out by irradiating silver carboxylate microcrystals by a UV lamp (continuous spectrum SVD-120A, 10^{-2} J/cm^2: short irradiation was for 3 min, extended irradiation was 15–20 min). The cross-section of partially decomposed silver carboxylate microcrystals was obtained by mixing $[Ag(O_2C_nH_{2n-1})]_2$ crystals with a polyvinylbutyral polymer, such as commonly used in photothermographic imaging materials,[1,2] in a special mold. After hardening, thin cuts, 1500–2500 Å thick, were made using a diamond blade microtome.

SEM and TEM investigations of the initial and decomposed $[Ag(O_2C_nH_{2n-1})]_2$ crystals were carried out using a JEM-2000FXII microscope equipped with a scanning ASID-20 device at an accelerating voltage of 200 kV. Ag^0 particle size estimates were made from analyzing approximately 600 particles from TEM photographs with Sigma Scan Pro version 3.0 (Jandel Scientific Software, 1996) software. For the preparation of suitable TEM samples, the $[Ag(O_2C_nH_{2n-1})]_2$ crystals were dispersed in a water–alcohol solution. A drop of the dispersion was then placed on a Cu TEM grid precoated with carbon film. After evaporation of the solution, the grids were introduced into the TEM on a cooling holder. All the operations were done under red light, including transportation and insertion into the microscope. These TEM studies used a liquid nitrogen single-tilt holder operating at its minimum temperature (–160°C) to avoid, as much as possible, radiation damage by 200 kV electrons. Most crystals could be observed for over an hour without any change under these conditions. For SEM observation, a thin gold film was thermally deposited on the samples in vacuum.

In order to study the thermal decomposition of silver carboxylates, *in situ* investigations of the structure and morphology changes occurring in $[Ag(O_2C_nH_{2n-1})]_2$ crystals during the decomposition were carried out directly in the electron microscope column. In order to do this, a small number of silver carboxylate crystals were placed on a W TEM grid, which was then placed on an electron microscopy heating stage, EM-SHH4, where the crystals were heated to the temperatures of interest, 120–180°C.

In addition to the electron microscopy studies, the changes in the composition of the silver carboxylate during decomposition were followed by means of x-ray phase analysis obtained on a DRON-4M diffractometer.

Results

Figure 1 shows scanning microphotographs obtained of the starting $[Ag(O_2C_nH_{2n-1})]_2$ crystals. As these photos show, all the silver carboxylate crystals, silver caprate (n = 10), laurate (n = 12), myristate (n = 14), palmitate (n = 16), stearate (n = 18), and behenate (n = 22), are plate- or needle-shaped. The length of silver carboxylate crystals is up to 2 μm, their width is about 0.2–0.4 μm and thickness is 0.1–0.2 μm. The size of silver carboxylate crystals decreases somewhat from silver caprate to behenate.

The x-ray diffraction patterns of the initial silver carboxylate samples provided the interlayer distance, $d_{(001)}$, depending on the number of carbon atoms in the methylene chain (Fig. 2). These values are in good agreement with the data reported elsewhere.[16,17]

Changes in Silver Carboxylate Structure and Phase Composition During Heating

X-ray Studies. X-ray studies of thermal decomposition of the silver carboxylates revealed similar changes occurring both in the silver carboxylate structure and in the formation of the metallic silver phase, regardless of the number of carbon atoms in the methylene chain (Fig. 3). Heating the crystals at 140–160°C for 30 min leads to a substantial decrease in the $d_{(001)}$ reflection intensity. The intensity of the hkl reflections (where h and k are not zero) also decrease substantially and broaden. For this heating time, the x-ray patterns do not show a metallic silver phase or any other phase forming. The metallic silver reflections, (111), (200) and (220), are observed in the x-ray patterns of the silver carboxylate heated at 140°C for 1 h for $[Ag(O_2C_{10}H_{19})]_2$ and for 2 h for $[Ag(O_2C_{22}H_{43})]_2$. These results are consistent with other literature reports relating thermal stability of silver carboxylates to chain length.[8,9,18] The $(111)_{Ag}$ reflection is significantly broadened. The $(200)_{Ag}$ and $(220)_{Ag}$ reflections can be identified only as a slight intensity increase at θ = 26°18' and 38°45' (Fig. 3).

In situ Electron Microscopy Studies of Silver Carboxylate Thermal Decomposition. The *in situ* investigation of silver carboxylate thermal decomposition directly in the column of the electron microscope showed that the heating of silver carboxylates is accompanied by changes in the appearance of the crystals, more specifically, the shape of the faces becomes round. The formation of a large number of particles, on the order of 1–2 nm, is observed within the silver carboxylate crystals (Fig. 4a). The selected area diffraction (SAD) pattern of this sample shows a set of diffusion rings characteristic of an amorphous material (Fig. 4b). An increase in the heating time is accompanied by coalescence of the silver particles formed which increases up to 3–5 nm. Electron diffraction patterns exhibit, along with the amorphous phase halo, the reflections characteristic of metallic silver (Fig. 4c). Prolonged heating of the silver carboxylate samples directly in the column of the electron microscope leads to a further increase of the metallic silver crystals. After heating $[Ag(O_2C_{18}H_{35})]_2$ crystals for 1 h at 170°C the silver crystallite size varies within rather wide range of 5 to 10 nm (Fig. 4d). The amorphous phase halo, which is characteristic of the initial stages of thermal decomposition, now essentially completely disappears

(a)

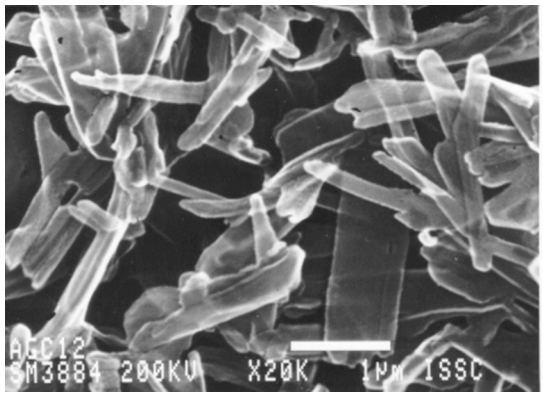

(b)

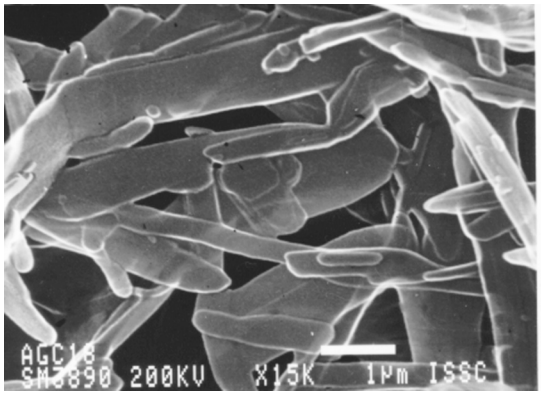

(c)

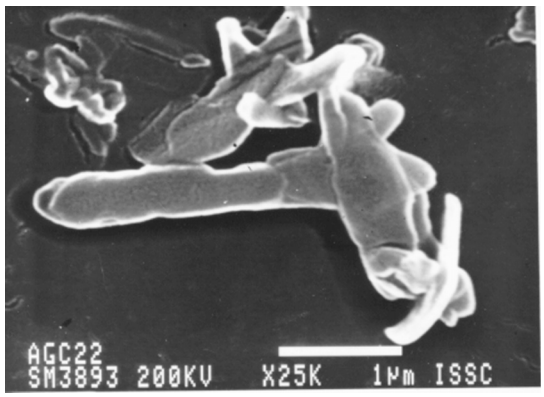

(d)

Figure 1. SEM of silver carboxylates – silver caprate (a), silver laurate (b), silver stearate (c) and silver behenate (d).

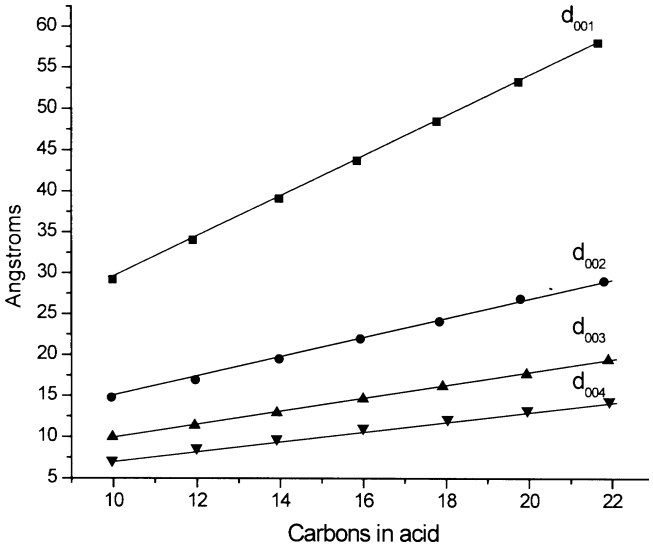

Figure 2. Dependence of interlayer distance, $d_{(00l)}$, in silver carboxylate structure on the number of carbon atoms in the methylene chain.

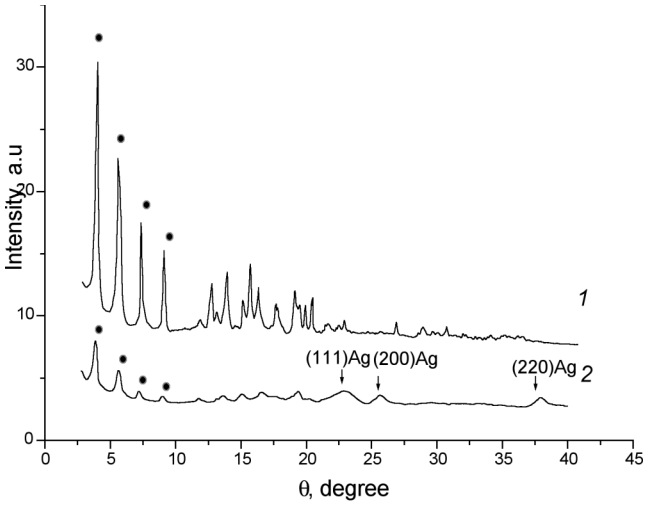

(a)

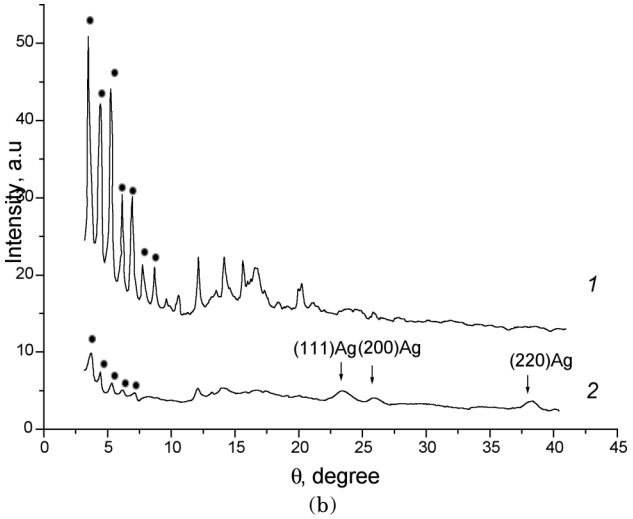

(b)

Figure 3. X-ray diffraction of heated silver carboxylates; silver caprate (a) and silver behenate (b), initial (1) and thermally decomposed at 160°C for 30 minutes (2). Dots denote the reflection data from the standard JCPDS file for the corresponding silver carboxylate.

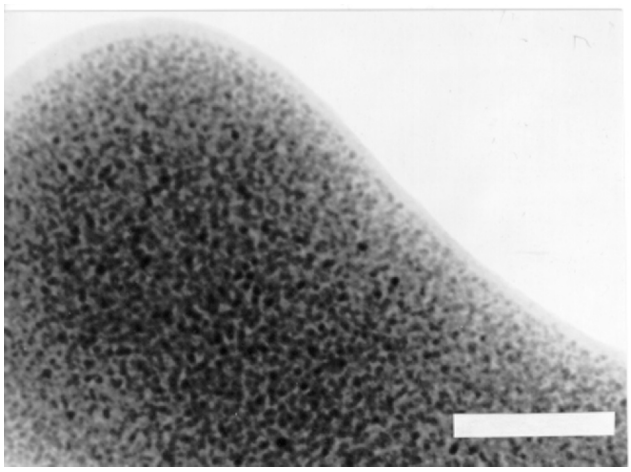

(a)

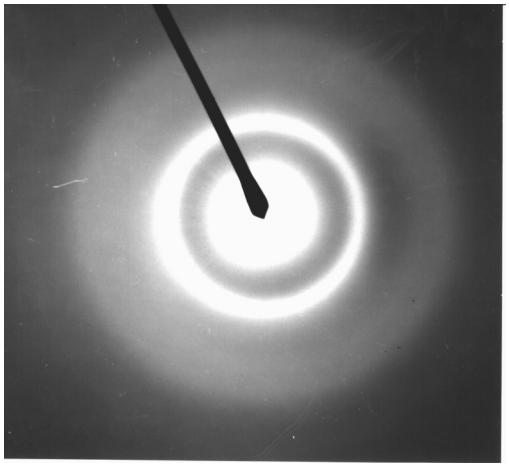

(b)

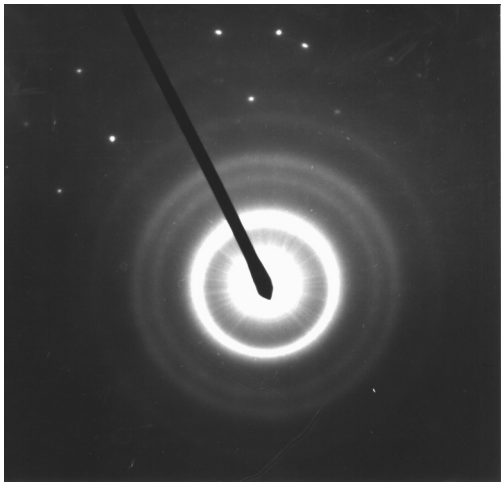

(c)

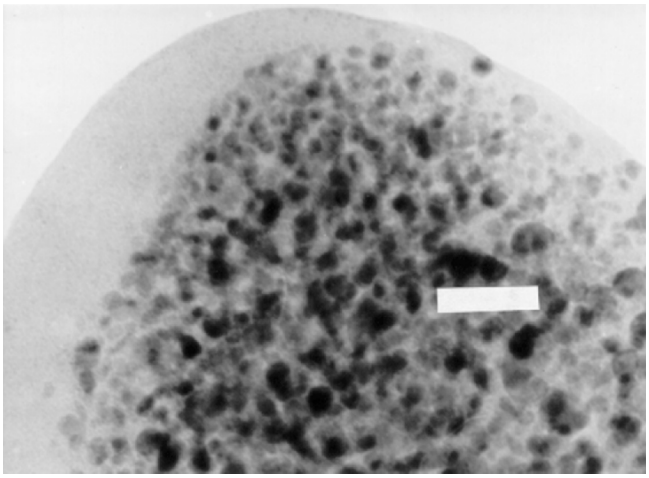

(d)

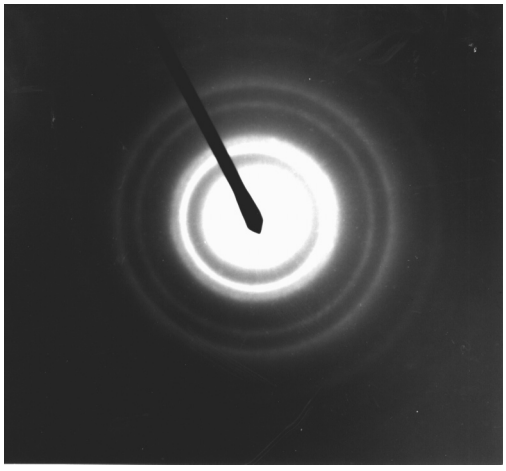

(e)

Figure 4. (a) Initial stage of AgC_{16} *in situ* thermal decomposition (scale marker is 50 nm); (b) SAD pattern of initial stage of decomposition of AgC_{16} at 140°C; (c) SAD of partially decomposed AgC_{10} showing the appearance of the metallic silver reflections; (d) TEM of AgC_{16} after prolonged *in situ* thermal decomposition (scale marker is 20 nm); and (e) SAD of decomposed silver palmitate heated at 140°C for 1 h.

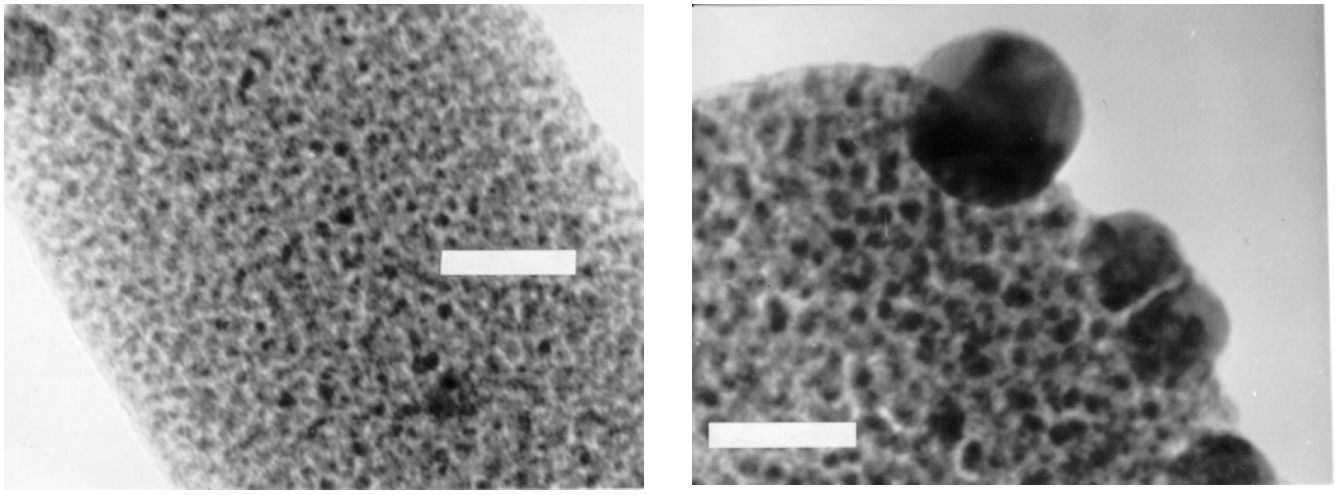

(a) (b)

Figure 5. (a) Formation of nano-sized silver particles in thermally decomposed AgC_{14} (scale marker is 20 nm); and (b) prolonged thermal decomposition of AgC_{10} – fine particles forming within the crystal and large particles on the lateral surface (scale marker is 20 nm).

and the reflections of the metallic silver crystal phase appear (Fig. 4c). However, it should be noted that at the same time the amorphous halo, having a maximum at d = 0.22 nm, disappears, a new halo appears, having a maximum at d = 0.32 nm (Fig. 4e). This latter halo is characteristic of amorphous carbon formation.[19,20] It should also be noted that the image of the decomposing silver carboxylate crystal shows an increase of the amorphous layer thickness at the edges of the crystal as the heating time increases. These results suggest that the formation of amorphous carbon during the thermal decomposition of carboxylate crystals is related to well-known contamination of electron microscope samples during heating and irradiation of hydrocarbon compounds.[21] It is expected that new hydrocarbon compounds form during the thermal decomposition of silver carboxylates along with the metallic phase formation. The destruction of these hydrocarbons by the electron beam leads to the deposition of carbon on the lateral faces of the decomposing $[Ag(O_2C_{18}H_{35})]_2$ crystal.

Electron microscope studies of the structure and morphology of silver particles formed during isothermal decomposition of silver carboxylates. The investigation of the structure and morphology of metallic silver particles formed during thermal decomposition of silver carboxylates showed that the sequence of silver particle formation is similar for all the silver carboxylates under investigation, the only difference is the time in which the structure and size changes are achieved.

While the formation of silver particles during isothermal decomposition of silver carboxylates is nearly identical to the sequence of silver particle formation stages occurring during *in situ* decomposition of silver carboxylates as described in the previous section, it should be noted that there are substantial differences. First, at the initial stages of silver carboxylate decomposition at 160°C, small particles are formed, on the order of 1–2 nm (Fig. 5a). Electron diffraction from these small particles is characterized by the superposition of an amorphous halo having a maximum of d = 0.22 nm. Increasing the decomposition time leads to an increase of the metallic silver particle size, up to 2–5 nm (see Fig. 5b), and the appearance of the diffraction pattern characteristic of silver particles. At the same time, the formation of silver crystals on the order of 5–10 nm is observed at the lateral faces of the silver carboxylate crystal (Fig. 5b). In the regions adjacent to a larger silver particle formed at a lateral face, the number of small silver particles is observed to decrease. However, extended heating, up to an hour, does not lead to the formation of large silver crystals within the decomposing silver carboxylate crystal. Under these conditions, only an increase in the number of silver crystallites formed at the lateral faces of silver car-boxylate crystals is observed.

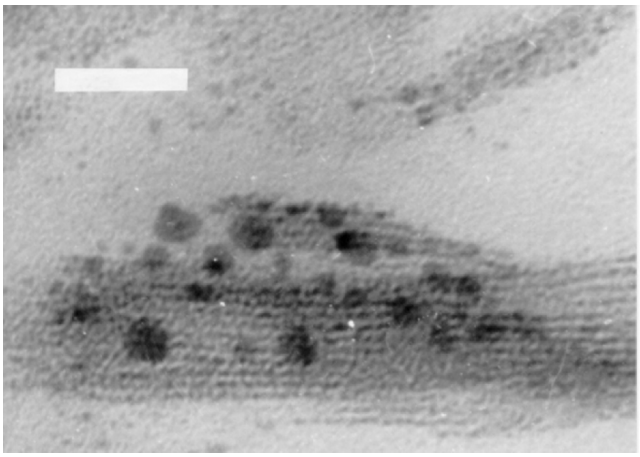

Figure 6. Layered precipitation of Ag particles of partially thermally decomposed silver carboxylate crystals (scale marker is 20 nm).

Additionally, the formation of silver particles during thermal decomposition of silver carboxylates was observed in cross sections of the crystals. Electron microscope studies of the sections of partially decomposed silver carboxylate crystals showed that the small silver particles (1–3 nm) formed during thermal decomposition are arranged in alternating layers, the distance between them being 3–5 nm. (Fig. 6).

In addition, electron microscope studies of isothermally decomposed silver carboxylate crystals showed

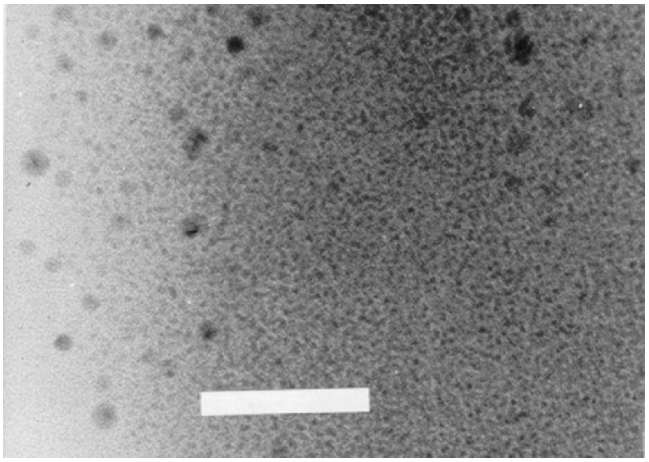

Figure 7. Initial stage of photochemical decomposition of AgC_{16} (scale marker is 50 nm).

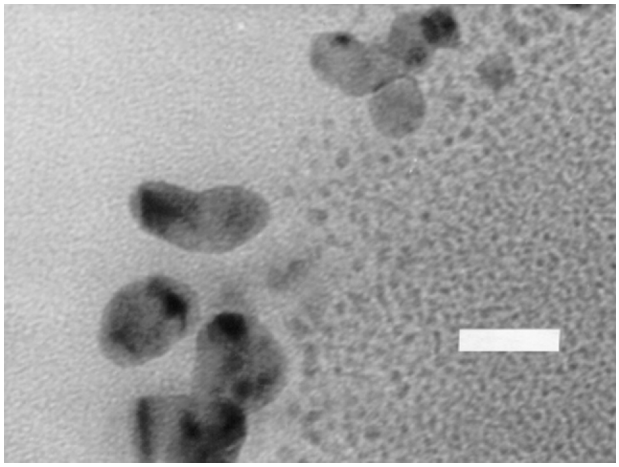

Figure 8. TEM of photochemically decomposed AgC_{16}, extended irradiation (scale marker is 20 nm).

that, unlike the case of *in situ* decomposition of silver carboxylate crystals when the amorphous carbon-containing phase was observed to grow on the lateral faces of crystals, the decomposition of crystals outside the column of the electron microscope does not lead to the formation of an amorphous phase and no amorphous halo of a carbon phase is observed in the electron diffraction patterns.

Electron Microscope Studies of the Structure and Morphology of Metallic Silver Particles Formed During Photochemical Decomposition of Silver Carboxylates

The investigation of the morphology of the silver particles formed during photochemical decomposition of silver carboxylates revealed that the sequence of stages leading to the formation of the silver phase during the photolysis of $[Ag(O_2C_{18}H_{35})]_2$ is generally similar to thermal decomposition. First, at low irradiation doses the formation of very small particles is observed (1–3 nm) (Fig. 7). Electron diffraction from these particles is characterised by the presence of an amorphous halo, similar to the cases described above. Then, increasing the irradiation dose causes a slight increase of the particle size (up to 3–5 nm) (Fig. 8). Electron diffraction patterns exhibit reflections characteristic of a bulk silver crystal phase. Analogous to thermal decomposition of silver carboxylates, silver particles are observed to form on the lateral faces of the crystal (Fig. 9). The size of these particles is somewhat larger than those particles formed inside the decomposing silver carboxylate crystal. Similar to thermal decomposition, a decrease in the number of small silver particles is observed in the regions adjacent to a large silver particle growing at the lateral face.

A feature of the morphology of the photochemical process distinguishing it from thermal decomposition of silver carboxylate crystals is the conservation of the appearance of the silver carboxylate crystals (Figs. 7 and 8). In this case, decomposition does not cause any significant change in the $[Ag(O_2C_{18}H_{35})]_2$ crystal habit.

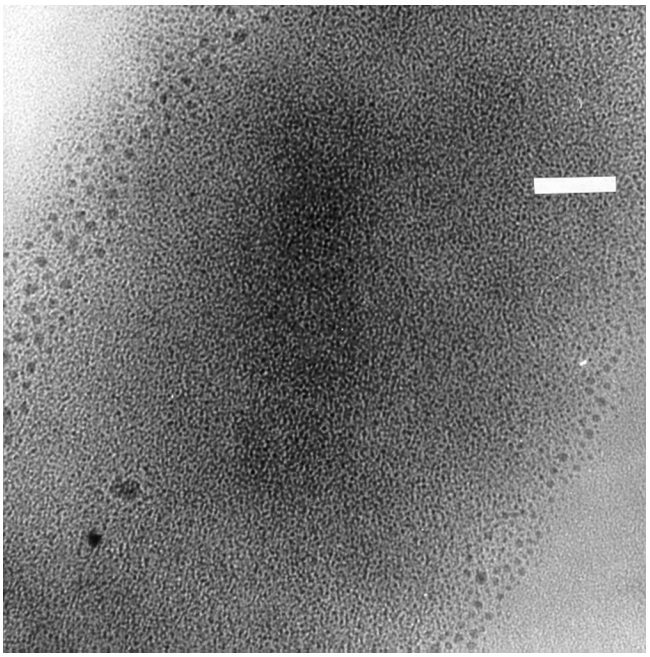

Figure 9. TEM of photochemically decomposed AgC_{16}. Silver particles form on the lateral faces of the crystal (scale marker is 50 nm).

Discussion

In order to understand the regularities observed for the morphology and structure of metallic silver particles formed during thermal and photochemical decomposition of silver carboxylates, it is necessary to consider the structure of the initial silver carboxylate crystals and its changes during heating.

It is known that the crystal class of all $[Ag(O_2C_nH_{2n-1})]_2$ silver carboxylates is triclinic, where n = 10–22, and contain two molecules per unit cell.[17] Recent structural studies of silver stearate showed that $Ag(O_2C_{18}H_{35})$ molecules form dimers, $[Ag(O_2C_nH_{2n-1})]_2$.[22] It can be seen from this structure that one of the most important features that can define the characteristics of the metallic silver particles formed during thermal and photochemical decomposition processes is the layered structure (Fig. 6) in which double layers of silver atoms are separated by hydrocarbon chains. The distance between double layers of silver atoms in the silver carboxylate structure depends on the number of carbon

atoms in the methylene chain and varies from 2.8 nm in silver caprate (n = 10) to 5.8 nm in behenate (n = 22), as shown in Fig. 2 and elsewhere.[16,17]

It is also known that silver carboxylates undergo several mesomorphous transformations during heating.[8,16,23,24] These phase changes are characterized by disorder in the methylene chain packing followed by disorder in the silver layers. It was also observed that in the sub-waxy state the decomposition of the silver carboxylate releases a portion of the silver ions as Ag atom radicals.[25]

The mechanism of thermal and photochemical decomposition of silver carboxylates proposed in the literature[25] assume that both processes involve similar stages:

$$Ag(O_2C_nH_{2n-1}) \longrightarrow Ag + C_{n-1}H_{2n-1}\cdot + CO_2$$

However, careful analysis of the literature [8,17,26] reveals differences in the thermal and photochemical decomposition. For example, unlike thermal decomposition of silver carboxylates that occurs in a mesomorphous phase, photochemical decomposition occurs in the crystal phase.

Taking the literature data and the current results into account we conclude that the solid state structure of the silver carboxylates is the primary factor that determines the structure and morphology of the metallic silver particles formed during decomposition, independent of decomposition conditions (thermal or photochemical). Thus, we found that nano-sized, amorphous metallic silver particles are formed (1–3 nm) at the initial stages of thermal and photochemical decomposition of silver carboxylates. The formation of these particles and subsequent growth of the silver phase occur within the silver atom layer in the silver carboxylate structure. Evidence of this is clearly demonstrated by the cross-sections of the decomposing silver carboxylate crystals (Fig. 6). It should be stressed that during thermal decomposition at 150°C the layered structure of the initial silver carboxylate crystal is maintained in spite of the fact that the silver carboxylates are in a mesomorphous state at this temperature. Silver behenate has been reported to be in a liquid crystalline phase at this temperature.[10] Photochemical decomposition is clearly observed to occur in the crystal state so that the silver phase can be formed only within the silver layer of silver carboxylate crystal. It is reasonable to conclude that the atomic silver formed during the decomposition of the silver carboxylates cannot diffuse through the substantial thickness of the double layers of methylene chains (approximately 45 Å for n = 18)[27] and is consistent with conductivity measurements of silver carboxylates.[24,28] It is most likely that the formation of the metallic silver phase occurs within the double silver layer. This is particularly likely when it is taken into account the fact that the Ag···Ag separation in the silver carboxylate dimer of $[Ag(O_2C_xH_{2x-1})]_2$ is typically 2.8 Å, the same as in metallic silver.[2,29] Thermal or photochemical combination into a Ag_2 dimer from this pre-organized arrangement can be easily envisioned and is consistent with EXAFS observations at elevated temperatures.[22] The mobility of silver atoms should be higher for thermal decomposition than for photochemical decomposition because of the higher temperature of silver carboxylate thermal decomposition.

We also conclude that the morphology of the silver particles formed during thermal and photochemical decomposition of silver carboxylates is affected by the formation of the organic reaction product, which could readily adsorb to the silver particle surface. While it is difficult to provide analytical evidence for this adsorption under these reaction conditions, it is well known that organic species readily adsorb onto metallic surfaces such as silver[30,31] including carboxylic acids.[32,33] In addition, in a separate investigation, the particle growth of metallic silver in the presence of a surfactant was found to be in competition with termination of growth due to surfactant coating on the silver particle.[34,35] Therefore, we conclude that adsorption of organic by-products on the metallic surface can be expected to influence the kinetics of silver particle growth.

Nano-sized silver particles formed during the decomposition possess excess surface energy, which can be compensated by increasing the particle size. The most convenient place for silver particles to grow, from the growth possibilities available, is on the lateral faces of the silver carboxylate crystals as these faces contain the available silver in the solid state structure of $[Ag(O_2C_nH_{2n-1})]_2$. The location of the silver ion layer in the solid state explains why silver crystallites grow on the lateral faces of the silver carboxylate crystals during thermal and photochemical decomposition, as shown in the figures. In addition, the concentration of nano-sized silver particles is observed to decrease in the regions adjacent to the lateral faces of crystal. In our opinion, this is good evidence of silver atom diffusion mobility during thermal and photochemical decomposition, as well as evidence of the tendency to compensate the excess surface energy of the silver particle. Furthermore, the nature of the metal particle formation during thermal and photochemical decomposition of silver carboxylates is similar to the formation of silver halide phase during the *in situ* halogenation of silver carboxylates reported previously.[36] In the latter case. it was shown that silver halide crystals are formed at the lateral faces of the $[Ag(O_2C_nH_{2n-1})]_2$ crystals. The AgX formation is also related to the layered structure of silver carboxylates and silver atom diffusion occurring only along the silver layers.

The formation of nano-sized amorphous particles observed at the initial stages of thermal and photochemical decomposition requires special consideration. Unfortunately, at present, it is difficult to detect the nano-sized amorphous silver particles at the very early stages of silver carboxylate decomposition. Additional investigation of the chemical and structural characteristics of these particles is necessary. It is very probable that the particles formed at this stage are silver particles. The small particle size (1–3 nm) and the small number of silver atoms comprising these particles is consistent with the amorphous halo observed in the diffraction patterns. It is well established[37] that nano-sized metal particles, including silver, can form non-equilibrium crystal structures even in the case of large sizes (about 5 nm). Just slight increases in the silver particle size to 3–5 nm leads to the appearance of x-ray diffraction characteristics of metallic silver and provides indirect confirmation of the metallic silver nature of these amorphous particles.

Comparison of the morphology and structure of silver particles formed during thermal and photochemical decomposition of pure silver carboxylates with the morphology of silver particles formed during thermal development of photothermographic materials shows good correlation to the size of silver particle crystals (3–5 nm). However, unlike thermal and photochemical decomposition of silver carboxylates where the metallic

silver particles are distributed inside the crystal, silver particles form a spherical aggregate (dendrite crystal) in the photothermographic process. It is likely that the differences in morphology of the silver particles formed in the photothermographic process are influenced by the presence of toning and developing compounds in the composition during thermal development. In fact, some of these components have been observed to form well-defined complexes with silver carboxylates.[38,39]

Conclusions

Thermal and photochemical decomposition of silver carboxylates leads to the formation of nano-sized silver particles (3–5 nm). This type of metallic silver formation can be directly attributed to the layered structure of the solid state structure of the $[Ag(O_2C_nH_{2n-1})]_2$ dimers in the crystalline lattice. The long hydrocarbon chains effectively confine movement of silver ions to the silver ion layer and hinder movement across the hydrocarbon layer to adjacent silver ion layers. In addition, this type of metallic silver formation is influenced by the organic by-products formed during decomposition. This can hinder the addition of silver atoms to the growing metal crystallite.

References

1. D. H. Klosterboer, Neblette's Eighth Edition: *Imaging Processes and Materials*, J. M. Sturge, V. Walworth, A. Stepp, Eds., Van Nostrand-Reinhold, New York, 279 (1989).
2. P. J. Cowdery-Corvan and D. R. Whitcomb, *Handbook of Imaging Materials,* A. Diamond, D. Weiss, Eds., Marcel Dekker, in press.
3. B. B. Bokhonov, L. P. Burleva and D. R. Whitcomb, *J. Imaging Sci. Technol.* **43,** 505 (1999).
4. Yu. E. Usanov, T. B. Kolesova, I. M. Gulikova, L. P. Burleva, M. R. V. Sahyun, and D. R. Whitcomb, *J. Imaging Sci. Technol.* **43,** 545–549 (1999).
5. B. B. Bokhonov, L. P. Burleva, D. R. Whitcomb, and M. R. V. Sahyun, *Microsc. Res. Technol.* **42,** 152 (1998).
6. B. B. Bokhonov, O. L. Lomovsky, V. M. Andreev, and V. V. Boldyrev, *J. Solid State Chem.* **58,** 170 (1985).
7. I. Geuens and I. Vanwelkenhuysen, *J. Imaging Sci. Technol.* **43,** 521 (1999).
8. V. M. Andreev, L. P. Burleva and V. V. Boldyrev, *Izv. Sib. Otd. Akad. Nauk SSSR, Ser. Khim. Nauk.* **5,** 3 (1984).
9. M. Ikeda, *Photogr. Sci. Eng.* **24,** 277 (1980).
10. I. Geuens, I. Vanwelkenhuysen, and R. Gijbels, *2000 International Symposium on Silver Halide Technology*, IS&T, Springfield, VA.
11. L. Bastin, C. Catry, I. Cupens, K. Jeuris, C. Jackers, F. De Schryver, and F. Ruttens, *2000 International Symposium on Silver Halide Technology*, IS&T, Springfield, VA.
12. S. Sugihara, A. Iwasawa, H. Tabei, and J-I. Yamaki, *Nippon Kagaku Kaishi.* **11,** 992 (1994).
13. Y. Yonezawa, Y. Konishi, H. Hada, K. Yamamoto, and H. Ishida, *Thin Solid Films* **218,** 109 (1992).
14. Y. Yonezawa, M. Kijima, *Nippon Shashin Gakkaishi* **56,** 3 (1993).
15. B. B. Bokhonov, L. P. Burleva, W. Frank, M. B. Mizen, M. R. V. Sahyun, D. R. Whitcomb, J. Winslow, and C. Zou, *J. Imaging Sci. Technol.* **40,** 417 (1996).
16. F. W. Matthews, G. G. Warren and J. H. Mitchell, *Anal. Chem.* **22,** 514 (1950).
17. V. Vand, A. Aitken and R. K. Campbell, *Acta Cryst.* **2,** 388 (1949).
18. R. Gotoh, M. Arizawa and N. Kajikawa, *Tr. Mezhd. Kongr. Poverk.-Akt. Veshch.* 7th, 2(II), 724 (1978).
19. L. L. Ban, *Surface and Defect Properties of Solids*, Vol. 1, J. M. Tomas, M. W. Roberts, Eds., p. 54–94, London: The Chemical Society 1972.
20. M. V. Berry and P. A. Doyle, *J. Phys. C* **6,** L6–L10 (1973).
21. P. B. Hirsch, A. Howie, R. B. Nicholson, D. W. Pashley, and M. J. Whelan, *Electron Microscopy of Thin Crystals*, London, Butterworths (1965).
22. B. P. Tolochko, S. V. Chernov, S. G. Nikitenko, and D. R.Whitcomb, *Nucl. Instr. Meth. Phys. Res. (A)* **405,** 428 (1998).
23. M. Chadha, M. E. Dunnigan, M. R. V. Sahyun, and T. Ishida, *J. Appl. Phys.* **84,** 887 (1998).
24. N. F. Uvarov, L. P. Burleva, M. B. Mizen, D. R. Whitcomb, and C. Zou, *Solid State Ionics* **107,** 1998, 31.
25. V. M. Andreev, L. P. Burleva, V. V. Boldyrev, and Yu. I. Mikhailov *Izv. Sib. Otdel. Acad. Nauk SSSR, Ser. Khim. Nauk.* **4,** 58 (1983).
26. V. M. Andreev, The investigation of the photochemical decomposition of silver carboxylates and their application to photomaterials, PhD Thesis, Novosibirsk, 1984.
27. A. E. Gvozdev, *Ukrain. Fiz. Zhur.* **24,** 1856 (1979).
28. N. G. Khainovskii, E. F. Khairetdinov and V. M. Andreev, *Izv. Sib. Otd., Akad. Sci. USSR, Ser. Khim. Nauk.* **5,** 34 (1985).
29. M. R. V. Sahyun, *J. Imaging Sci. Technol.* **42,** 23 (1998).
30. B. Vlčková, X. J. Gu, D. P. Tsai, and M. Moskovits, *J. Phys. Chem.* **100,** 3169 (1996).
31. M. Muniz-Miranda and G. Sbrana, *J. Raman Spec.* **27,** 105 (1996).
32. W. S. Sim, P. Gardner and D. A. King, *J. Phys. Chem.* **100,** 12509 (1996).
33. W. S. Sim, P. Gardner and D. A. King, *J. Phys. Chem.* **100,** 30 (1996).
34. F. Mafune, J-y. Kohno, Y. Takeda, T. Kondow, and H. Sawabe, *J. Phys. Chem. B* **104,** 8333 (2000).
35. F. Mafune, J-Y. Kohno, Y. Takeda, T. Kondow, and H. Sawabe, *J. Phys. Chem. B* **104,** 9111 (2000).
36. B. Bokhonov, L. Burleva, W. C. Frank, J. R. Miller, M. B. Mizen, M. R. V. Sahyun, D. R. Whitcomb, J. M. Winslow, and C. Zou, *J. Imaging Sci. Technol.* **40,** 85 (1996).
37. K. Heinemann, M. J. Yacaman, C, Y. Yang, and H. Poppa, *J. Cryst. Growth* **47,** 177 (1979).
38. D. R. Whitcomb and R. D. Rogers, *Inorg. Chim. Acta* **256,** 263 (1997).
39. D. R. Whitcomb and R. D. Rogers, *J. Chem. Cryst.* **25,** 137 (1995).